NASA CONTRACTOR REPORT

NASA CR-159513

PREMIX FUELS STUDY APPLICABLE TO DUCT BURNER CONDITIONS FOR A VARIABLE CYCLE ENGINE

By K. S. Venkataramani

Prepared by

GENERAL APPLIED SCIENCE LABORATORIES, INC.

Westbury, New York 11590

For Lewis Research Center

NAS3-20603

NATIONAL AERONAUTICS AND SPACE ADMINISTRATION, WASHINGTON D.C.

DECEMBER 1978

TABLE OF CONTENTS

LIST OF FIGURES

INTRODUCTION

Currently, emissions and performance estimates for premixed duct burners suitable for a variable cycle engine require extrapolation of experimental data obtained at high inlet temperature levels into the range of temperatures near and below the fuel vaporization temperature. Furthermore, assumptions regarding the ability to achieve mixture homogeneity comparable to that of research burners are required before the extrapolated values from high inlet temperature test data can be utilized for performance evaluation.*

This report describes a brief experimental program in which the emission levels and performance of a premixing Jet-A/air combustor were measured at reference conditions representative of take-off and cruise for a variable cycle engine. Tests were also conducted at inlet temperatures of 400, 500 and 600K and reference Mach numbers of 0.117 and 0.087 in which the equivalence ratio was varied from 0.9 to the lean stability limit. Table I summarizes the test conditions at which data were obtained.

*A description of the variable cycle engine test bed program and the premixed duct burner test parameters can be found in Reference (1).

TABLE I

DEFINITION OF OPERATING CONDITIONS FOR PREMIX FUEL STUDY

1. Take-off (simulated VCE)

Equivalence ratio	.68 (vary ± .1)
Reference Mach Number	.117
Inlet-air Temperature, ^{o}K	430
Inlet Pressure, psia	39.3

2. Cruise (simulated VCE)

Equivalence Ratio	.68 (vary ± .1)
Reference Mach Number	.087
Inlet-air Temperature, ^{o}K	604
Inlet pressure, psia	36.8

3. Parametric variation at an inlet pressure of 38 psia

Equivalence ratio .9 to lean blowout
inlet-air temperatures of 400, 500 and 600K
Reference Mach number of .117 and .087

APPARATUS AND TEST PROCEDURE

Test Rig - The premixing combustion test rig is illustrated schematically in Figure (1). Heated dry air enters the apparatus through the contraction and passes through an instrumentation spool where the entrance temperature and pitot-static pressure profiles are measured by an instrumentation rake. Fuel enters the device through a plenum chamber which feeds a ring injector having eight 0.38 mm diameter orifices which discharge liquid jets normal to the air flow. The premixing passage is 30 cm long and 7.62 cm in diameter. Four thermocouples mounted 90° apart near the exit plane of the mixer tube serve as flashback/autoignition indicators. The combustor section employs an 80% blockage perforated plate flameholder attached to a 10 cm diameter stainless steel liner. The combustor assembly is supported within a heavy outer pressure vessel and is cooled by an auxiliary supply of cold air which is injected around the periphery of the liner. The combustor is provided with a sonic exit orifice and the rig pressure is controlled by a dome-loaded pressure regulator which supplies the cooling air. An integral hydrogen-air igniter is used to initiate combustion.

Fuel System - The fuel supply system is illustrated schematically in Figure (2). Jet-A fuel is stored in a tank and pressurized with nitrogen. The liquid is withdrawn from the lower portion of the supply tank and passed through a turbine flowmeter and pressure regulator. A cavitating venturi downstream of the pressure regulator in the fuel supply line maintains a constant flow rate independent of downstream pressure fluctuations.

Instrumentation - During emissions testing, gas samples were withdrawn from the combustor using the gas sampling rake illustrated in Figure (3). The rake contains seven 1.6 mm diameter sampling tubes supported within a water-cooled body. The sampling ports are located at 0, ±1.45, ±2.9 and ±4.35 cm measured from the combustor centerline. Water enters the rake through the hollow stem flowing forward to the head where it is exhausted through a number of 0.20 cm diameter holes in the narrow gap between the head and the two deflector plates. The exhausted water is thus used to convectively cool the deflector plates and film cool the rake head. A small portion of the water is

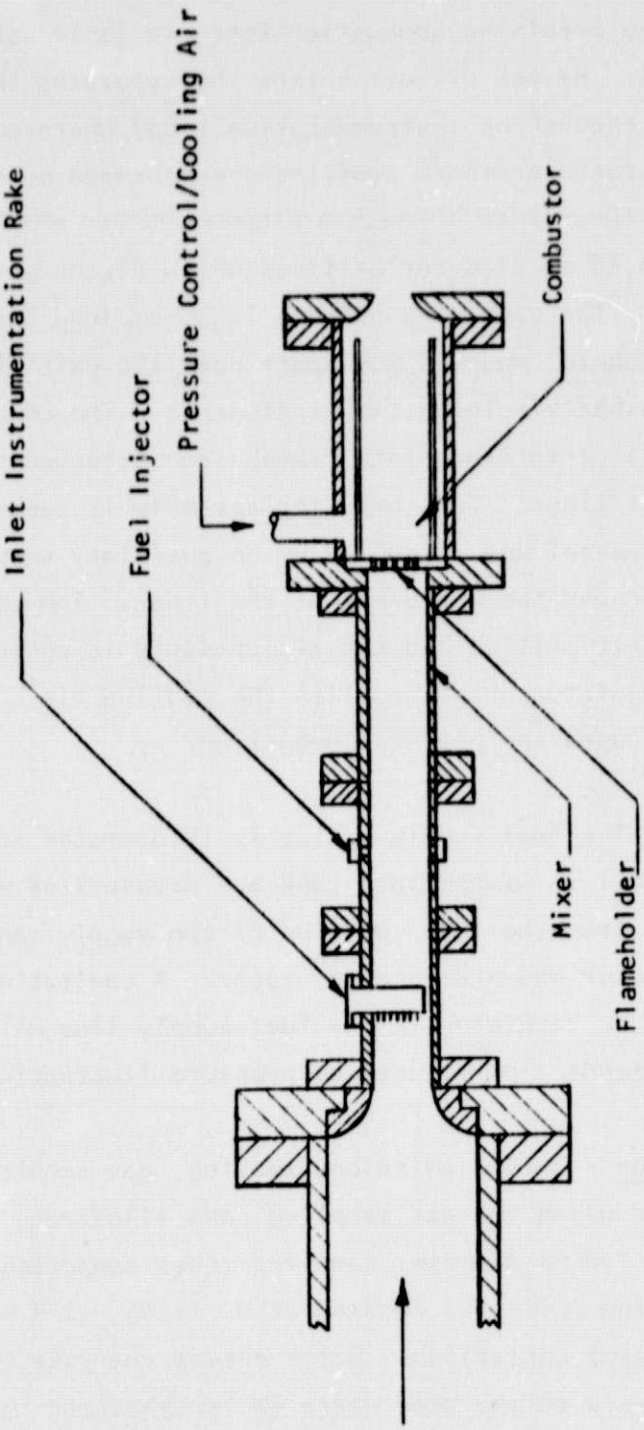

FIGURE 1. DUCT BURNER TEST RIG

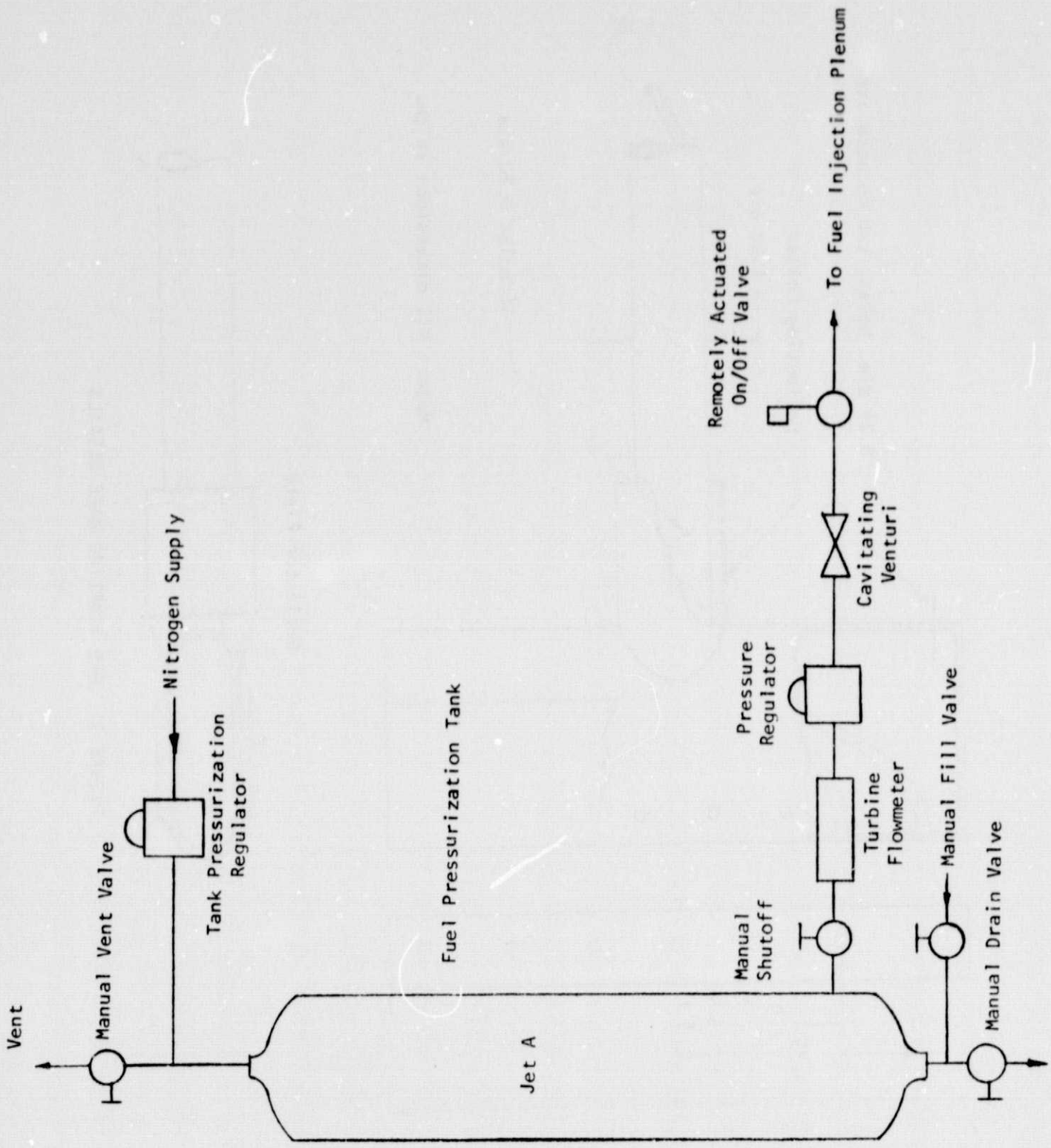

FIGURE 2. FUEL STORAGE AND DELIVERY SYSTEM SCHEMATIC

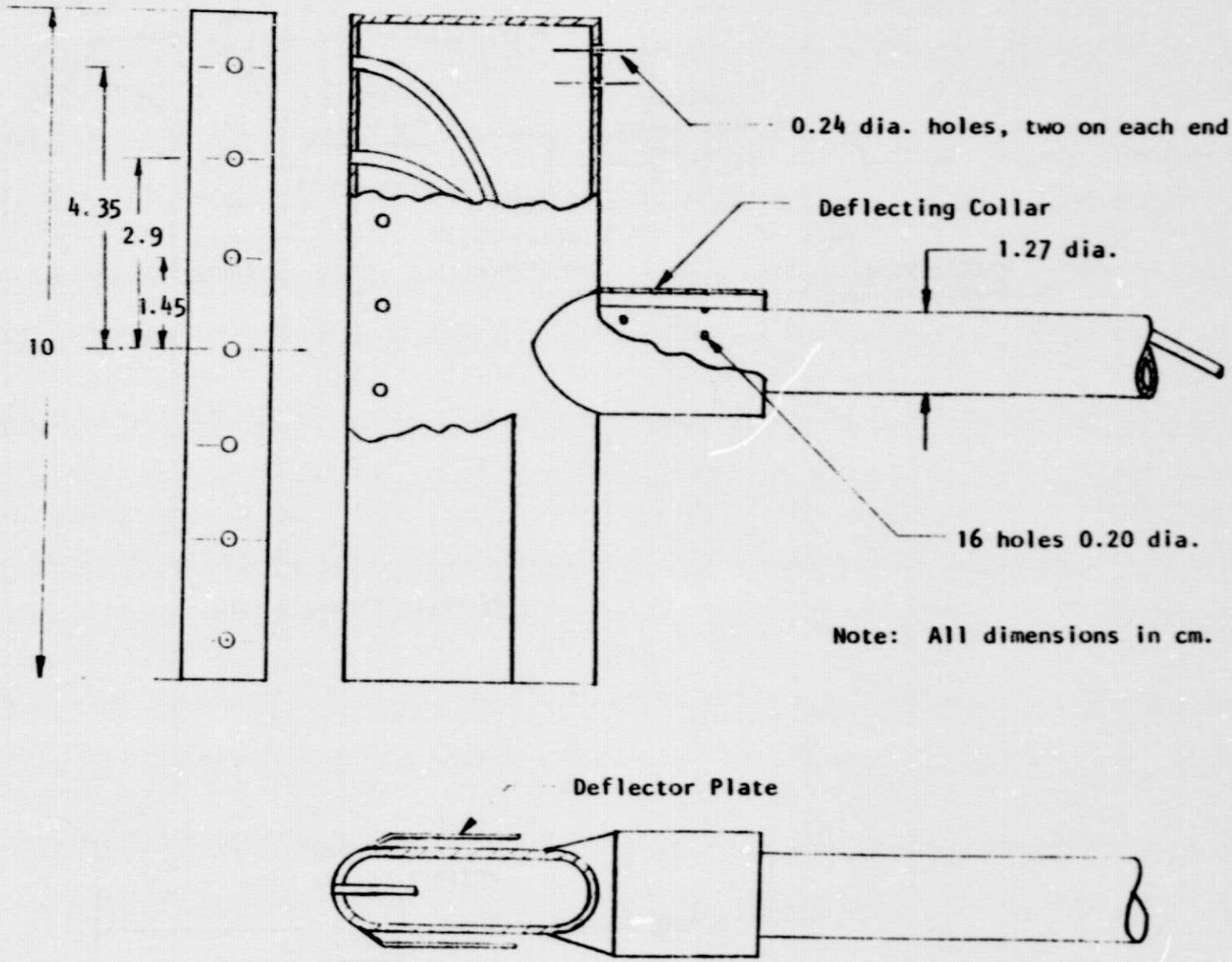

FIGURE 3. GAS SAMPLING RAKE DETAILS

exhausted through a set of 0.76 mm diameter holes in the hollow stem near the head junction to fill the space between the stem and a deflection collar, film cooling the upstream portion of the stem. Four 0.24 cm diameter holes located on the back of the rake exhaust a portion of the water which then impinges directly on the exit orifice plate thus providing it with additional cooling.

Captured gas samples are transported to a set of gas analyzers through stainless steel sampling lines which are heated to 175°C to prevent condensation of hydrocarbon species. The details of the gas analysis system and the data reduction equations are presented in the Appendix. The sampling rake was positioned 25 cm downstream of the flameholder exit station for all emission tests.

Air inlet conditions are monitored using an array of pitot tubes and thermocouples mounted in the inlet instrumentation spool which also contains two static pressure taps. The fuel plenum is provided with a pressure tap to monitor the pressure drop across the injector.

Test Procedure - In operation, the air flow through the rig was established at the required temperature and at a flow rate corresponding to the reference Mach number at the desired entrance pressure and temperature. The rig pressure was then brought up to the operating value by the injection of an appropriate amount of auxiliary air at the exit orifice. The gas igniter was then turned on, fuel flow initiated and slowly increased until ignition was achieved. The rig equivalence ratio was brought to the value desired for the particular test sequence, the gas igniter shut off and the rig operated for several minutes to assure steady conditions before withdrawing the gas sample.

For the take-off and cruise conditions, tests were run at three equivalence ratios. At each setting, a survey of emissions was made across the combustor by withdrawing gas samples from the individual ports of the sampling rake. For the parametric variation tests, the sample lines were manifolded to give a single averaged gas sample.

Progressively reducing the equivalence ratio during the parametric variation tests eventually caused the flame to blow out. Conditions at this point are defined as those corresponding to the lean stability limit. At some reference conditions, it was necessary to terminate the test prior to reaching the lean stability limit in order to avoid contamination of the gas sampling instrumentation due to excessive hydrocarbon emissions.

RESULTS

Prior to emissions testing, the fuel distribution produced by the eight-orifice ring injector and 30 cm premixing tube was measured along two mutually perpendicular diameters just upstream of the flameholder at the cruise operating condition. Samples were withdrawn through a pitot-type traversing probe and passed thorugh a catalytic reactor for oxidation prior to gas analysis. Equivalence ratio of the reacted sample was then determined as outlined in Appendix A.

The measured cruise-condition fuel distributions are presented in Figure (4) and indicate a substantial degree of nonuniformity at the combustor entrance with fuel tending to concentrate near the walls. Previous tests of the same fuel mixture preparation section (detailed in Reference 2) conducted at similar airstream conditions but far lower equivalence ratios produced fuel distribution profiles which were nearly the reverse of those obtained here with fuel then heavily concentrated near the centerline. Clearly, the fuel dispersion produced by the simple eight orifice ring injector is quite sensitive to operating condition with the higher fuel flow rates in the present experiment producing greater penetration of the liquid jets which may remain substantially coherent until they are turned downstream.

Surveys of emission levels across the combustor were carried out for the take-off and cruise conditions at three equivalence ratios. The variation of the emission indices across the combustor for the take-off condition is shown in Figure (5). In this and the following figures, CO emission data is not plotted since the concentration of CO at all test conditions was above the 5000 ppm maximum range of the infrared analyzer. In addition, as the CO levels could not be measured directly, it was necessary to employ the metered fuel/air ratio to convert emissions measurements.

The results shown in Figure (5) indicate that emission levels are not uniform across the combustor for the take-off condition indicating a nonuniform distribution of gas phase fuel. While unburned hydrocarbon levels increase moderately with increasing equivalence ratio, the corresponding increase in NO_x levels is quite small.

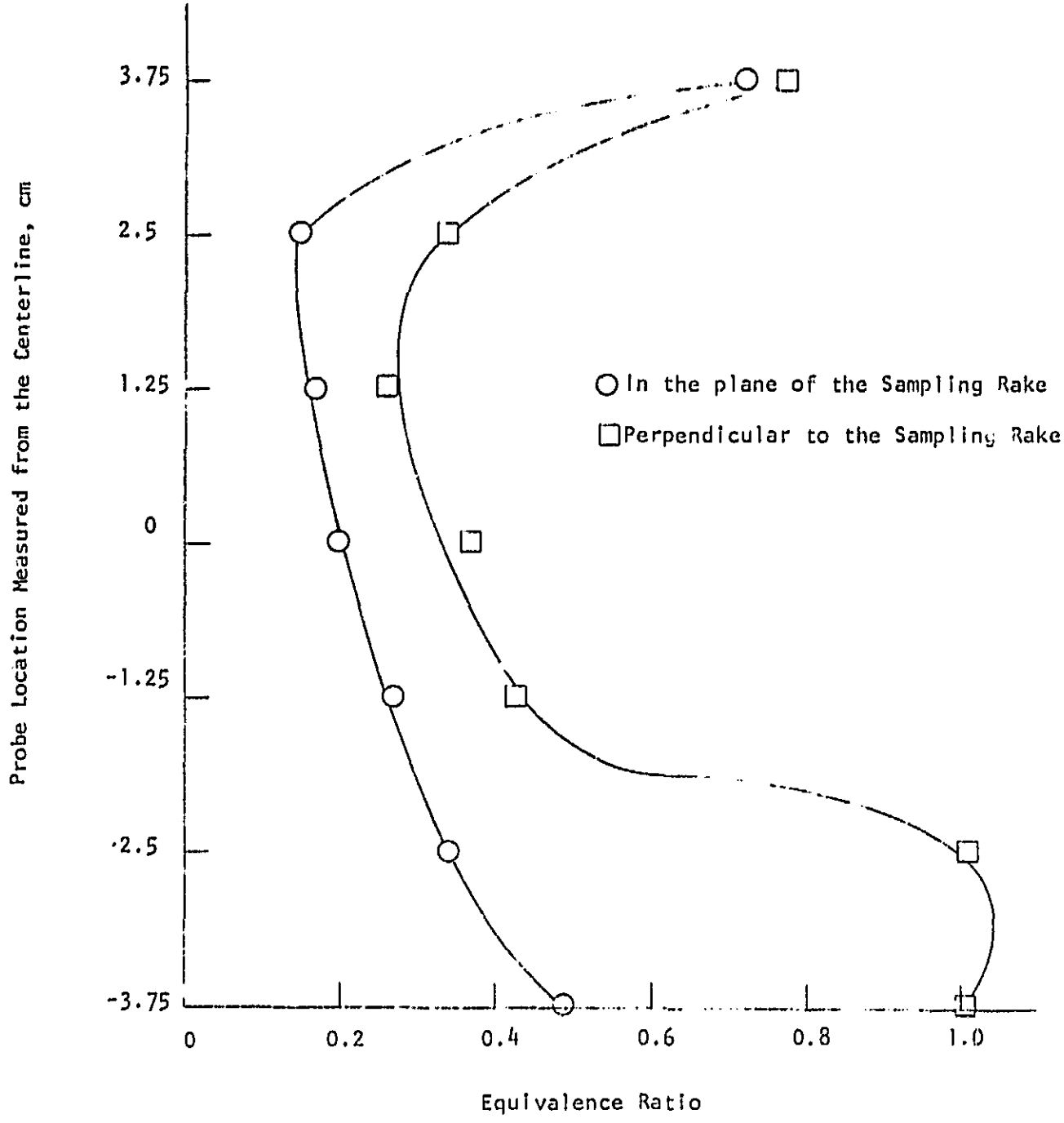

FIGURE 4. FUEL/AIR DISTRIBUTION UPSTREAM OF THE FLAMEHOLDER
Metered Equivalence Ratio = 0.68
Reference Mach Number = 0.087
Inlet Pressure = 36.8 psia Inlet Temperature = 604 K

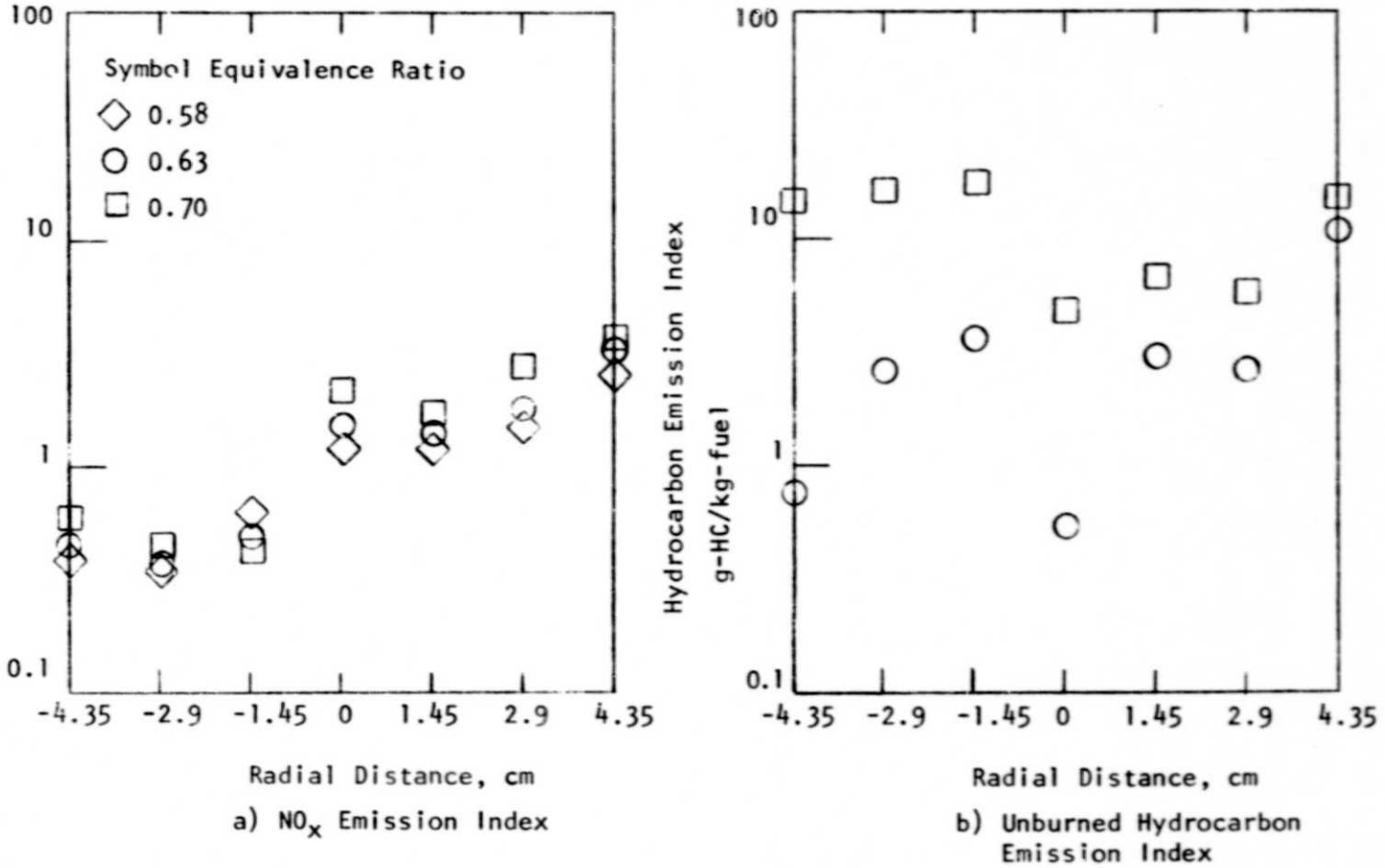

FIGURE 5. EMISSIONS SURVEY AT TAKE-OFF CONDITION
M_{ref}=0.117

The emissions survey results for the cruise condition are summarized in Figure (6). Here, the nonuniformity in hydrocarbon emission level is not as pronounced as at the take-off condition. As the equivalence ratio is increased from 0.54 to 0.76, the unburned hydrocarbon levels first decrease slightly and then increase whereas the NO_x levels generally decrease with increasing equivalence ratio. The unburned hydrocarbon levels at the cruise condition are approximately ten times larger than those at the take-off condition.

The parametric variation test results are plotted in Figures (7) through (12). At reference conditions of 600 K/M_{ref} = 0.117 and 500 K/M_{ref} = 0.117, the NO_x levels initially increase with equivalence ratio, reach a plateau and from there on decrease at a slow rate. At the same reference temperatures, but at a reference Mach number of 0.087, the NO_x levels decrease with equivalence ratio. At a reference temperature of 400 K, there appears to be very little influence of either reference Mach number or equivalence ratio on NO_x level.

Table II presents observed lean stability limits for the various inlet conditions. The lean stability limit equivalence ratio is lower at the higher Mach number at all the three reference temperatures. It is likely that this is due to better atomization at the higher fuel flow rate with a consequent reduction in time required for vaporization of the fuel droplets. The rather low values of the lean stability limit obtained at reference temperatures of 500 K and 600 K reflect the inefficient premixing characteristic of the mixture preparation element at these operating conditions.

TABLE II

OBSERVED EQUIVALENCE RATIO AT LEAN STABILITY LIMIT

$T_{inlet,K}$ \ M_{ref}	0.117	0.087
600	<0.35	0.4
500	0.3	0.44
400	<0.48	0.5

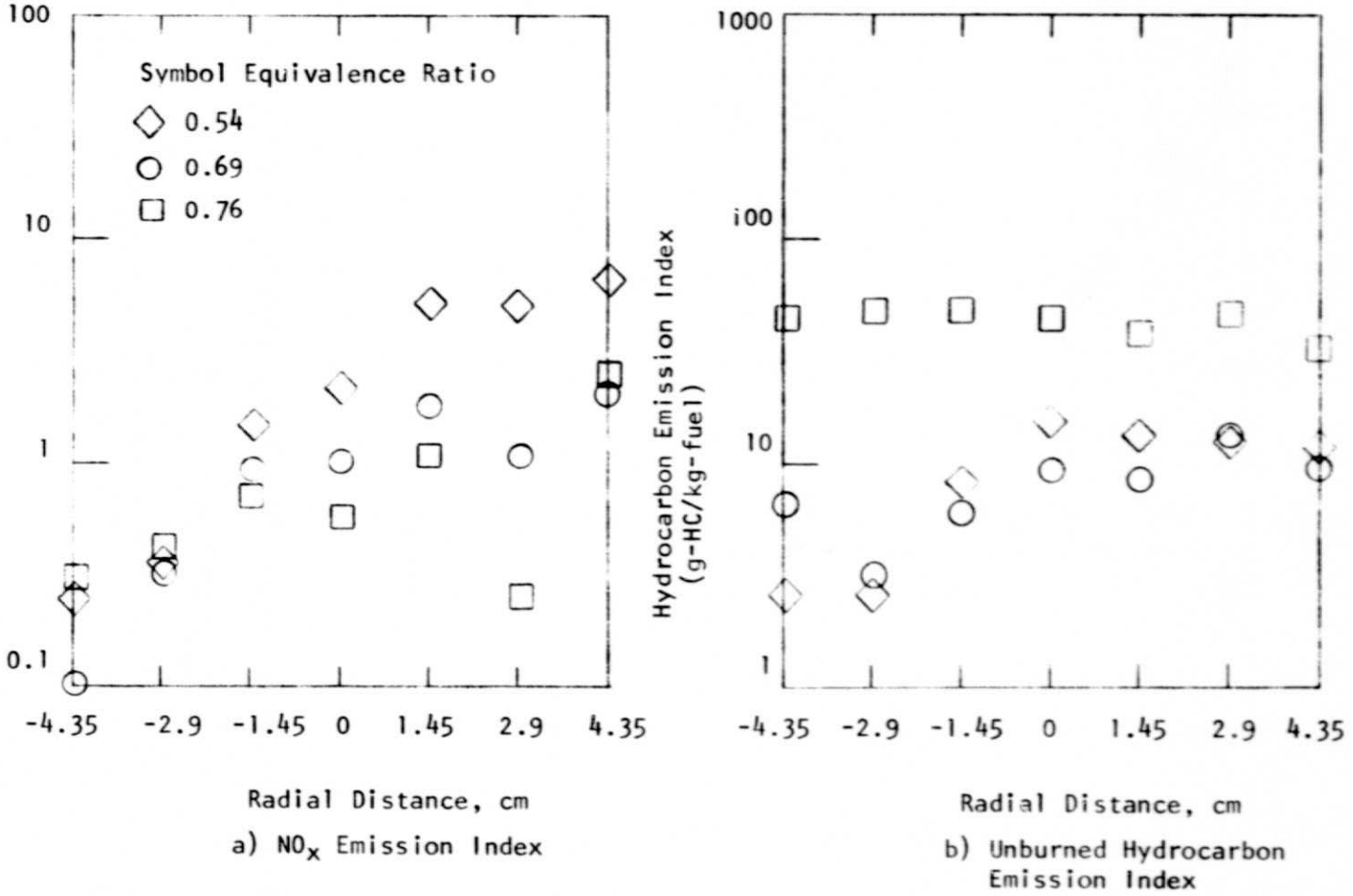

FIGURE 6. EMISSIONS SURVEY AT CRUISE CONDITION
M_{ref}=0.087

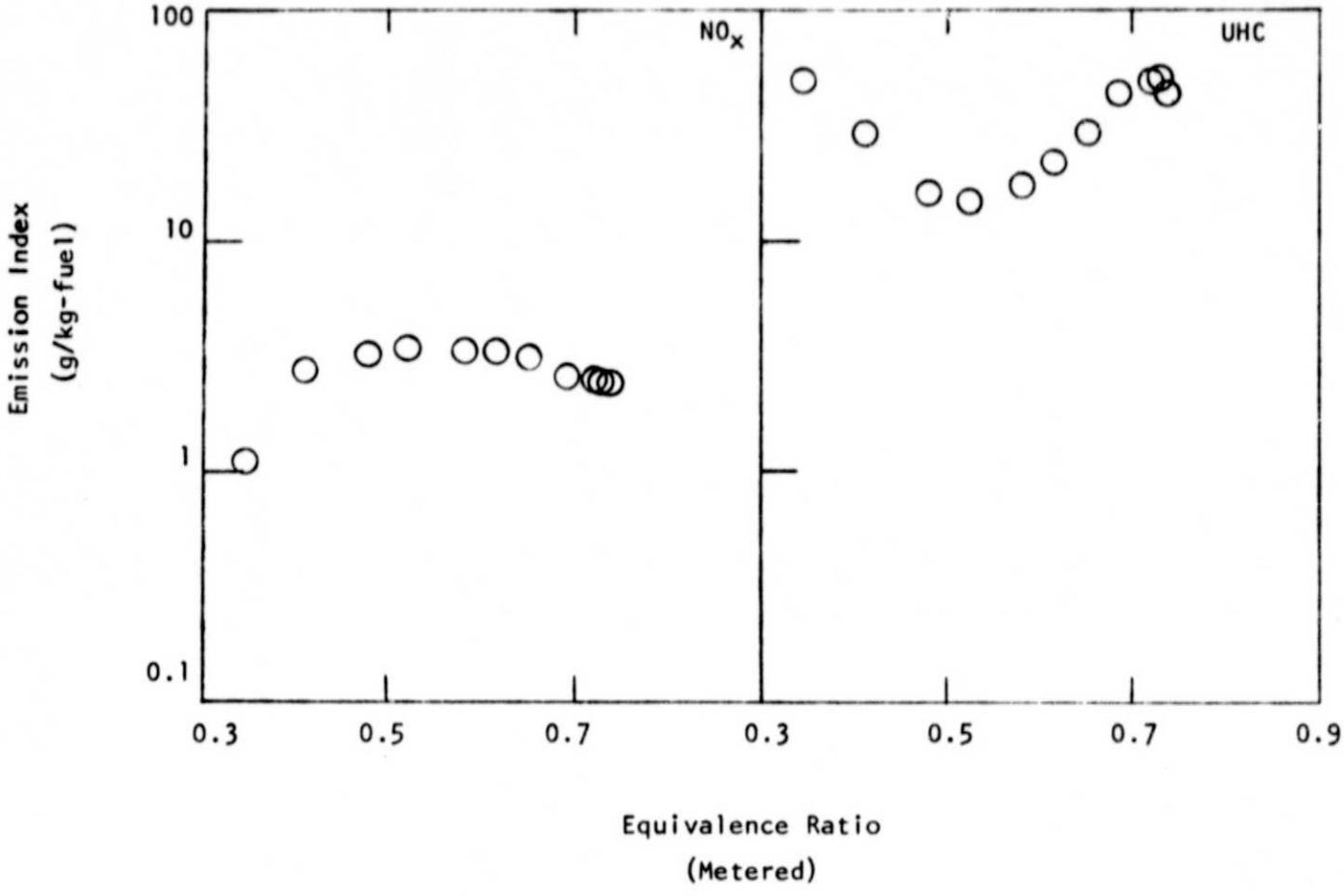

FIGURE 7. PARAMETRIC VARIATION EMISSION RESULTS

T_{ref}=600°K; M_{ref}=0.117

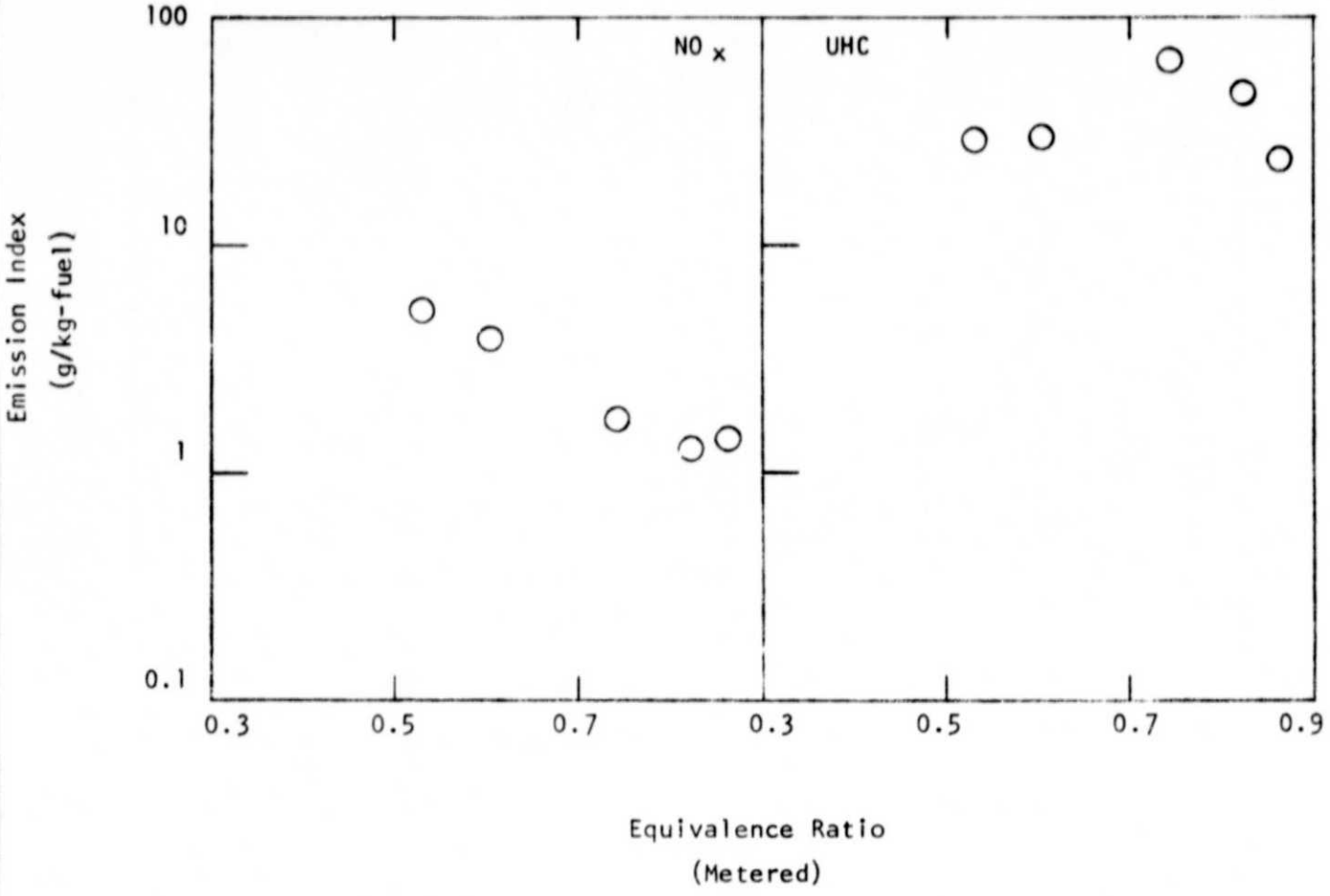

FIGURE 8. PARAMETRIC VARIATION EMISSION RESULTS

T_{ref}=600°K; M_{ref}=0.087

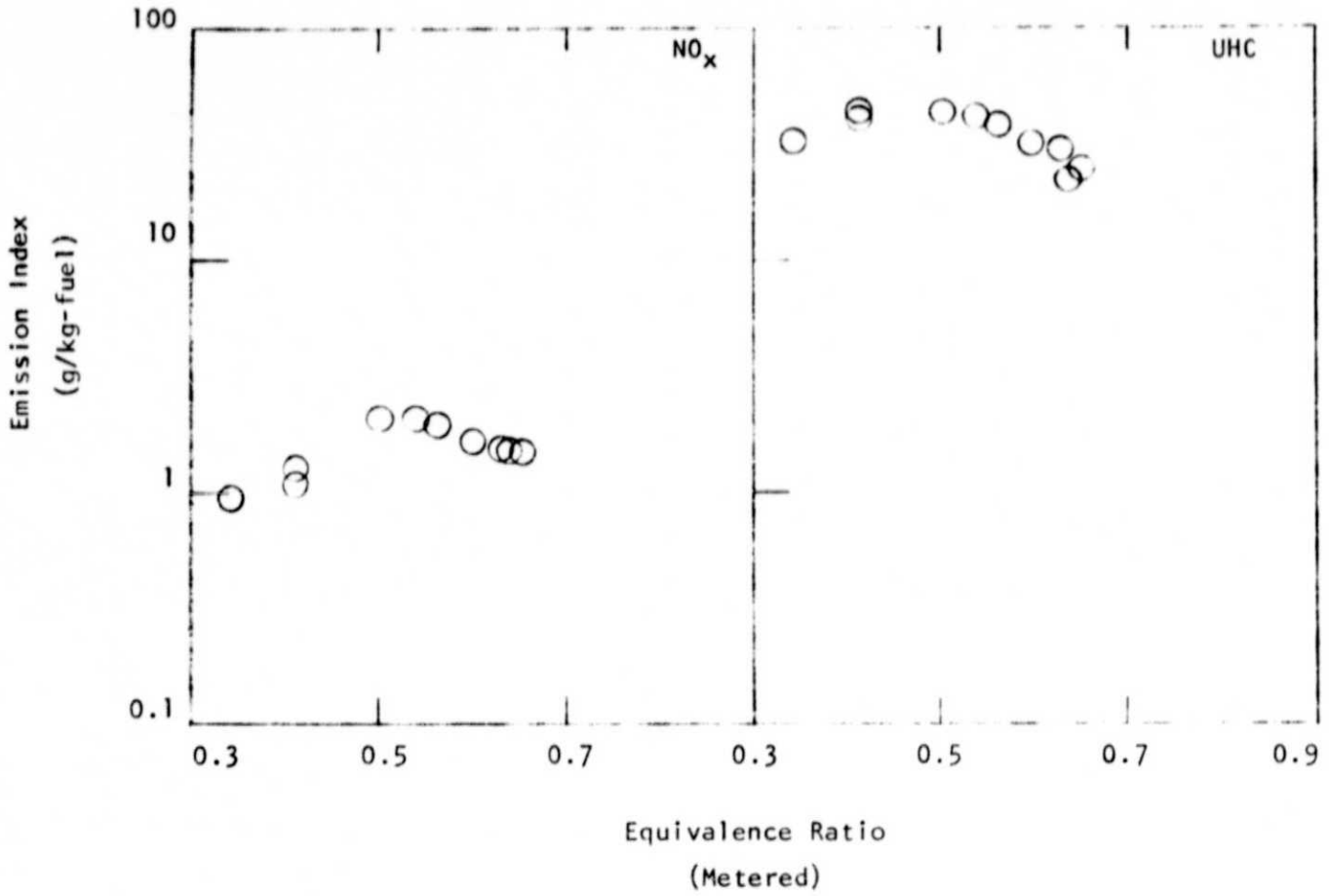

FIGURE 9. PARAMETRIC VARIATION EMISSION RESULTS

T_{ref}=500°K; M_{ref}=0.117

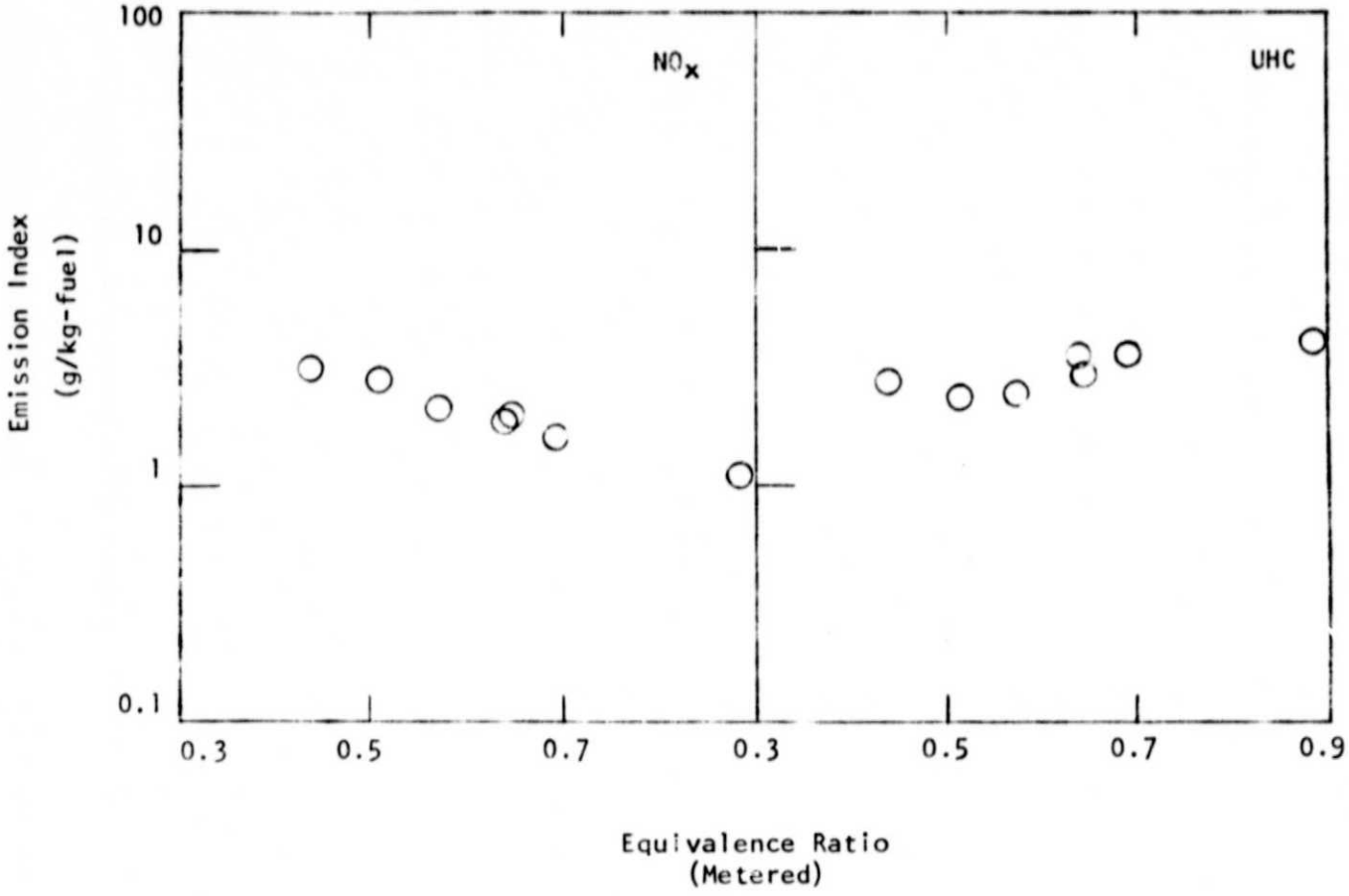

FIGURE 10. PARAMETRIC VARIATION EMISSION RESULTS

T_{ref}=500°K; M_{ref}=0.087

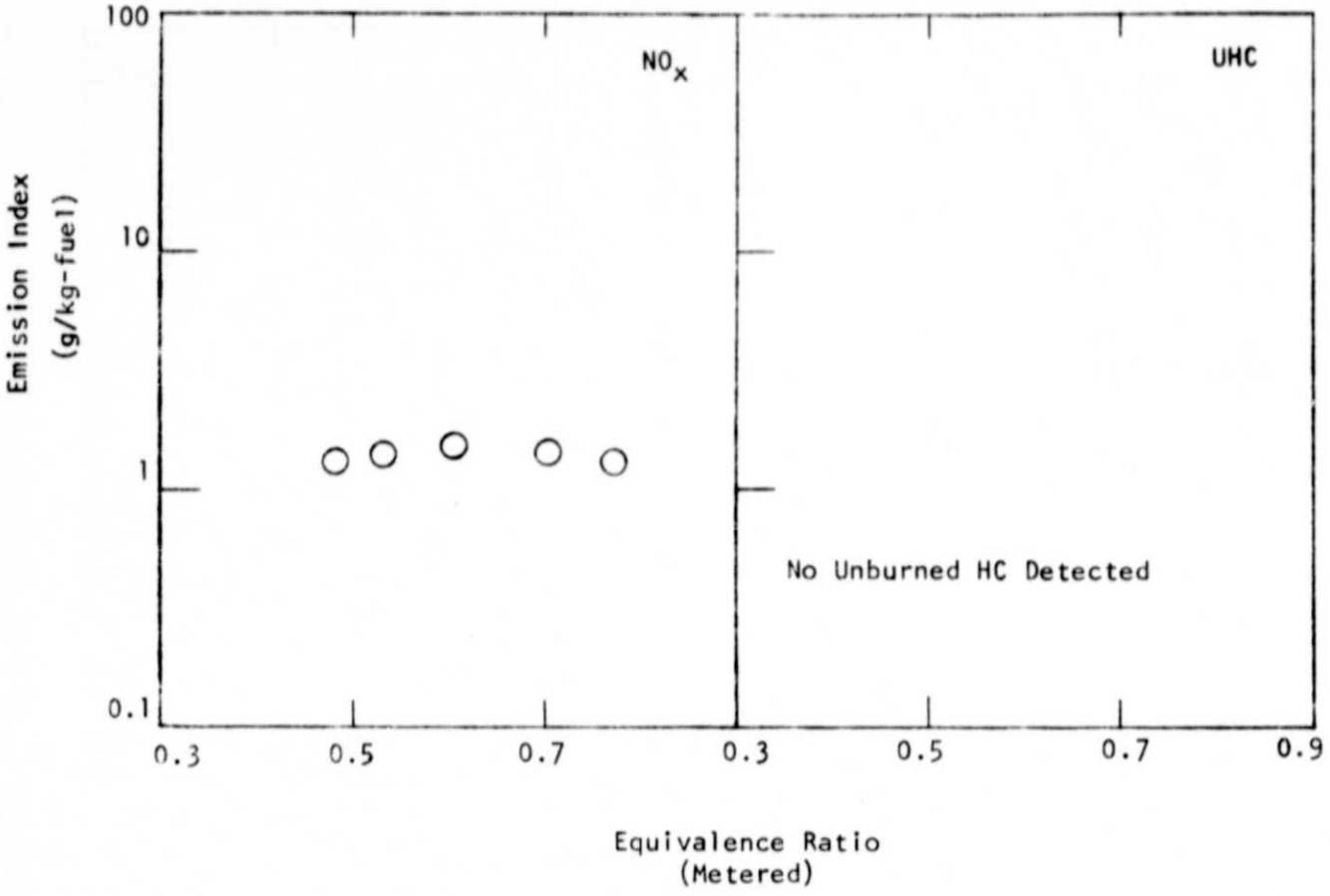

FIGURE 11. PARAMETRIC VARIATION EMISSION RESULTS

T_{ref}=400°K; M_{ref}=0.117

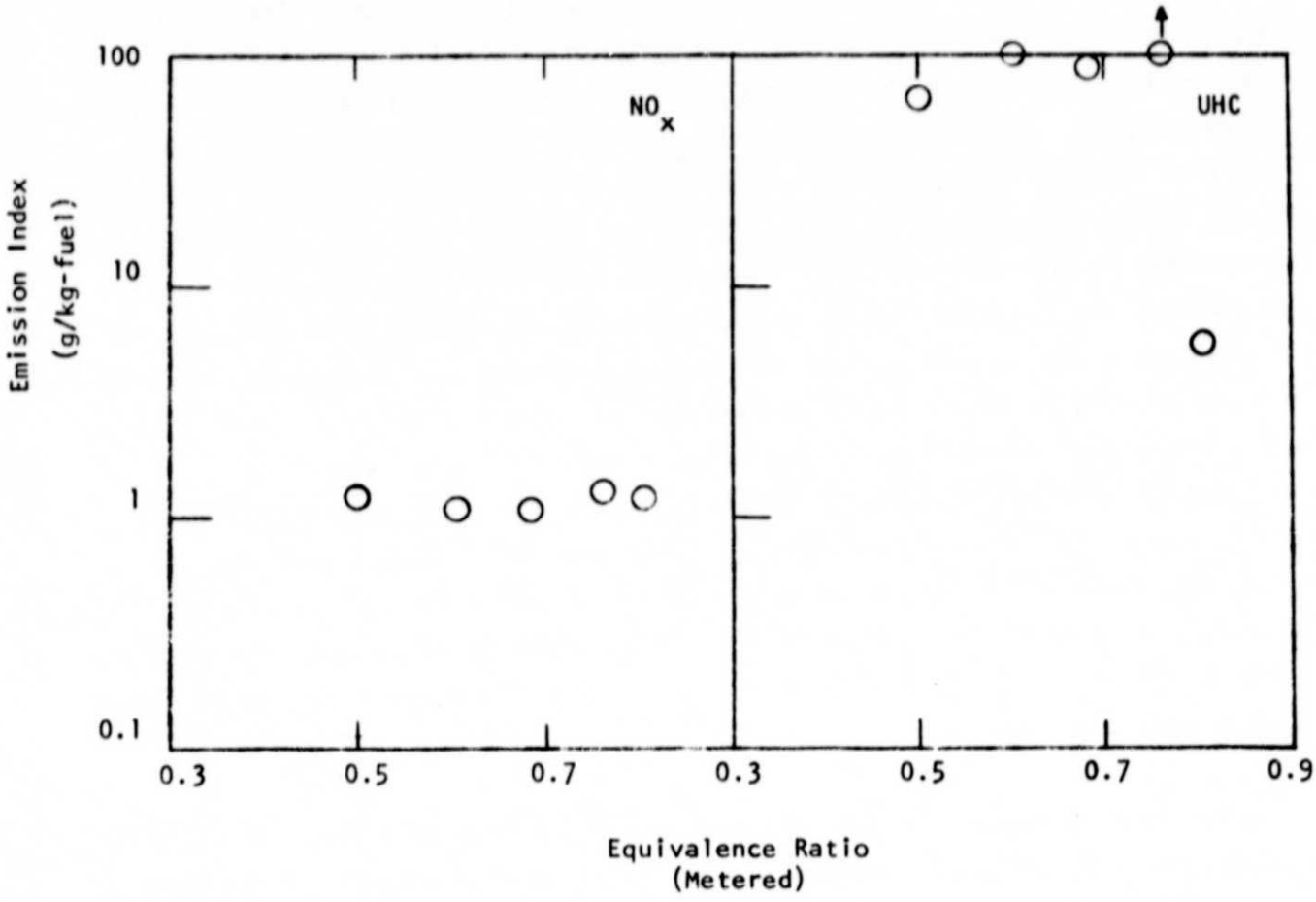

FIGURE 12. PARAMETRIC VARIATION EMISSION RESULTS

T_{ref}=400°K; M_{ref}=0.087

DISCUSSION

The cruise-condition fuel distribution profiles presented in Figure (4) indicate that the pressure atomizing ring injector does not produce a uniform fuel-air mixture under the current set of operating conditions. The large concentration of fuel near the walls suggests that the liquid jets issuing from the fuel nozzles remain coherent for a significant portion of their residence time within the mixer section. This is probably a result of the fact that the fuel injection pattern produced by a pressure-atomizing ring injector varies with fuel flow rate. Since the injector was originally designed to operate at approximately half the current fuel flow rate, the higher injection velocities used here would appear to have produced excessive penetration of the liquid jets. This conclusion is qualitiatively in conformity with penetration studies of water jets injected normally into a high velocity airstream, where the radial penetration distance was found to be proportional to $(U_{jet}/U_{air})^{0.95}$ (Reference 3). Calculations based on Reference (3) indicate that under conditions encountered in the present test program, the fuel jets penetrate nearly as far as the opposite wall. Significant accumulation of liquid phase fuel on the walls can occur under these circumstances and will considerably reduce the degree of prevaporization which can be achieved within a given duct length.

Emission levels measured at the take-off condition display a significant variation across the combustor, confirming a non-uniform distribution of gas phase fuel. While the unburned hydrocarbondistribution at cruise is more uniform than at take-off, NO_x level does not show a similar approach to uniformity.

In the parameteric variation sequence, a striking difference is observed in the NO_x emission characteristics when the reference Mach number is reduced from 0.117 to 0.087. At M_{ref}=0.117, NO_x levels initially increase with equivalence ratio, reach a maximum and then decrease at a slow rate. At the lower reference Mach number, NO_x levels decrease continually with equivalence ratio. This behavior is discernible at inlet temperatures of both 500K and 600K. At an inlet temperature of 400K, neither equivalence ratio nor reference Mach number has any observable influence on NO_x emissions.

Previous studies of premixed prevaporized combustion systems (Reference 4, e.g.) have shown that NO_x emission index for a premixed system correlates well with adiabatic flame temperature. In particular, NO_x emission index has been found to increase exponentially with this parameter. Since an increase in equivalence ratio at a given reference condition corresponds to an increase in adiabatic flame temperature, one would expect NO_x emission index (in parametric variation tests) to increase monotonically with equivalence ratio. The present results, however, do not display such a trend; in fact the results at 500K and 600K/M_{ref}=0.087 show just the opposite behavior. This discrepancy implies a sharp decrease in combustion efficiency with increasing fuel flow rate. As noted earlier, the fuel jets at the low reference Mach number condition apparently remain coherent producing increasingly poorer atomization as fuel flow is increased.

In Figure (13), the NO_x emission levels at 600K and 500K/M_{ref}=0.087 are plotted as a function of the measured CO_2 level. In both cases, NO_x levels increase exponentially with CO_2 which is a function of effective gas phase equivalence ratio. The behavior of the NO_x emission index illustrated in Figures (8) and (10) can therefore be attributed to incomplete vaporization. Considering the tests at M_{ref}=0.117 which show an increase of NO_x with equivalence ratio it would appear that the system behaves as an LPP combustor at low fuel flow rates where the higher relative velocity between the airstream and the fuel jet produces better atomization and less penetration. Increasing the fuel flow rate beyond a certain value appears to adversely affect the atomization process causing the gas phase equivalence ratio to drop from that point on. Due to the relatively high fuel flow rates and the low temperature involved, the 400K tests do not display sensitivity to change in the reference Mach number. At this inlet temperature, the gas phase equivalence ratio remains essentially constant over the entire range of metered fuel-air ratio.

With regard to CO and total hydrocarbons, the observed high concentration of these species provide additional evidence of poor vaporization and incomplete combustion. Since CO concentration at all parametric variation test conditions

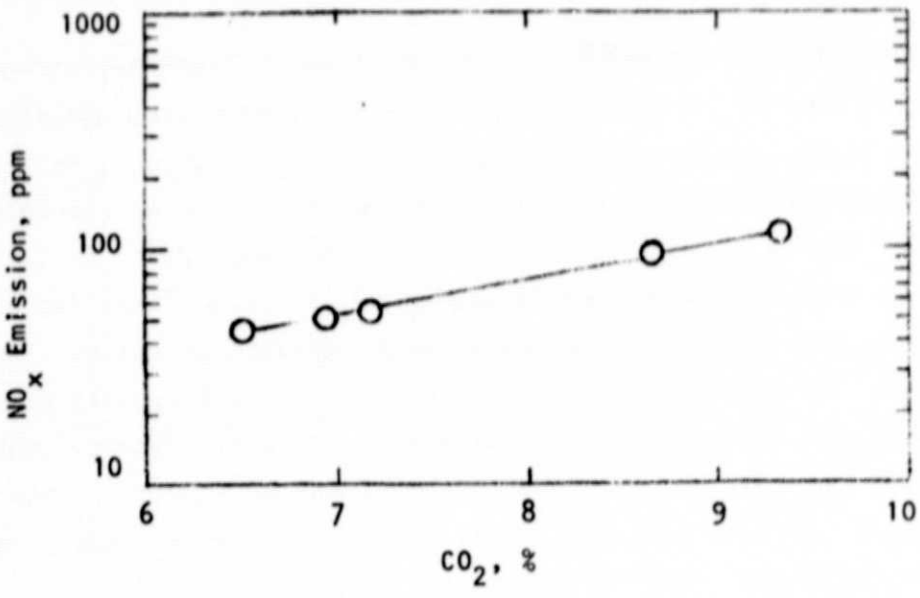

(a) $M_{ref} = 0.087$; $T_{ref} = 600K$

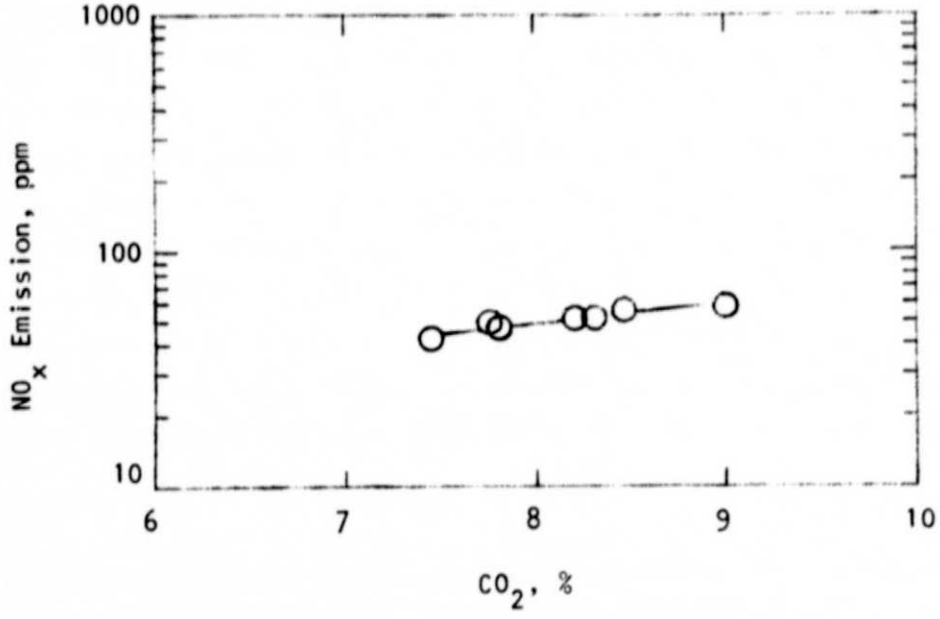

(b) $M_{ref} = 0.087$; $T_{ref} = 500K$

FIGURE 13. NO_x EMISSION AS A FUNCTION OF CO_2

was above the 5000 ppm maximum range of the infrared analyzer, a maximum theoretical combustion efficiency can be calculated based on a 5000 ppm level of CO. This maximum combustion efficiency is plotted in Figure (14) as a function of the parameter PT/V. For PT/V values from 2.23×10^6 to $3.36/\times 10^6$ $NsKm^{-3}$, the maximum combustion efficiency first increases with increasing PT/V, reaches a peak and then falls with further PT/V increase. Increased combustion efficiency with increasing PT/V is to be expected on the grounds that flame temperature increases with T and residence time increases with (1/V). The point at which the theoretical maximum combustion efficiency begins to deviate from this trend corresponds to the $M_{ref} = 0.087$ and $T_{ref} = 600K$ test condition and represents the lowest mass flow condition. It is likely that poor injector performance at this condition is responsible for the observed reversal in trend.

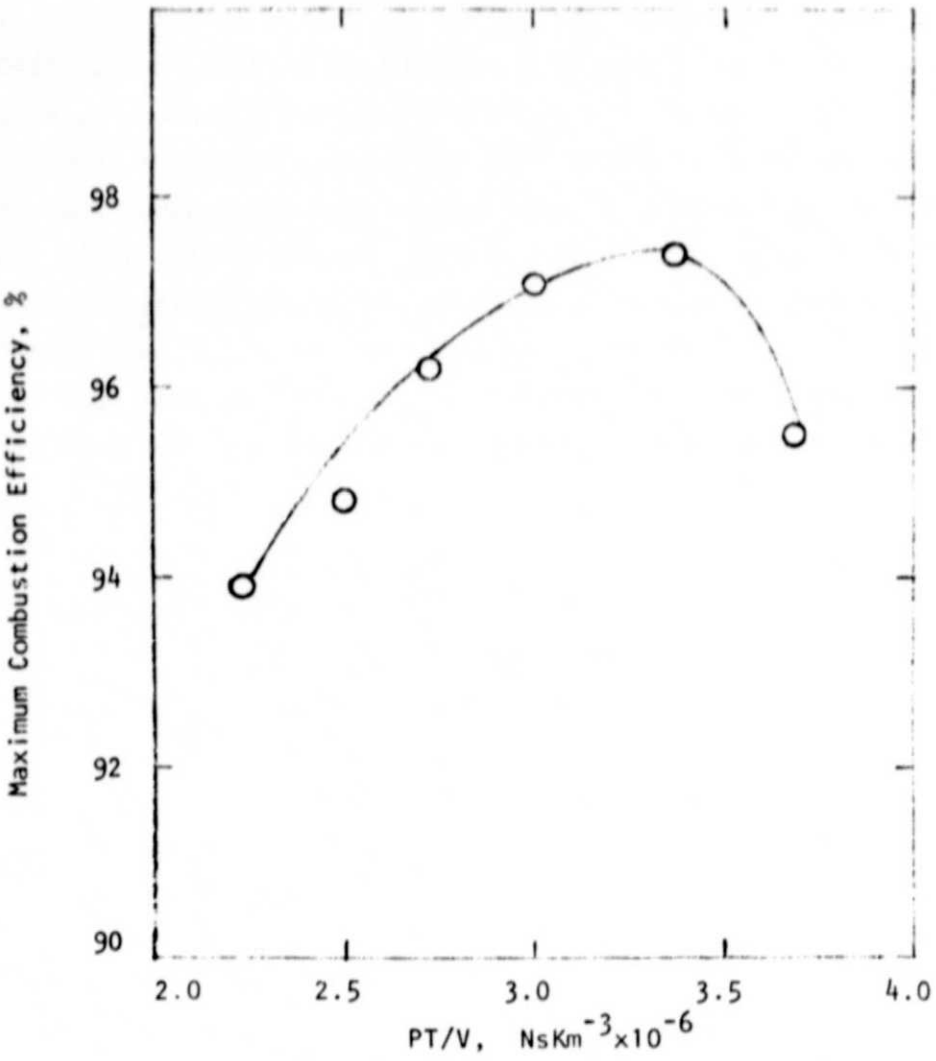

FIGURE 14. VARIATION OF MAXIMUM COMBUSTION EFFICIENCY (BASED ON 5000 PPM CO) WITH INLET CONDITIONS

SUMMARY OF RESULTS

i) Ignition was achieved at all reference conditions.

ii) Fuel distribution tests upstream of the flameholder revealed significant concentration of fuel near the walls of the premixing duct. Uniform premixing was not achieved under the present operating conditions and fuel distribution profile appears to be sensitive to fuel flow rate (and hence to equivalence ratio).

iii) Carbon monoxide emission levels were greater than 5000 ppm at all operating conditions.

iv) Emission levels at the take-off condition exhibited significant nonuniformity across the combustor cross section.

v) Unburned hydrocarbon levels across the combustor at the cruise condition were nearly ten times larger than at the take-off condition. The nonuniformity of the unburned hydrocarbon levels at the cruise condition was less pronounced than at the take-off condition.

vi) At a reference Mach number of 0.117 and at inlet temperatures of 500K and 600K, the NO_x emission levels initially increased with equivalence ratio, reached a plateau and then decreased slowly. The NO_x levels for the same inlet temperatures at a reference Mach number of 0.087 decreased with increasing equivalence ratio. At an inlet temperature of 400K, neither the reference Mach number nor the equivalence ratio had a perceptible influence on the NO_x levels.

vii) The lean blow-off equivalence ratio was lower at the higher reference Mach number for all three inlet temperatures.

APPENDIX A

DATA REDUCTION PROCEDURES

The gas analysis instrumentation provides raw data in the form of volume fractions of the particular gases being sampled. This raw data is converted into the more convenient form of emission index and equivalence ratio following the procedures detailed below.

Each of the gas analysis instruments must be calibrated in order to convert the instrument reading to the volume fraction of the particular gas being analyzed. This calibration is accomplished by passing prepared mixtures of calibration gas through the instruments and establishing calibration curves. The hydrocarbon analyzer was calibrated using gas standards containing 1040 ppm and 99 ppm propane in nitrogen. The instrument output is proportional to the number of carbon atoms with hydrogen bonds. Thus, pure hydrogen or pure carbon will produce no response and a given concentration of propane (C_3H_8) will produce three times the response of an equal concentration of methane (CH_4). The instrument responds to all C-H bonds. As a result, it measures the sum of both unoxidized hydrocarbon and partially oxidized hydrocarbon molecules. The instrument calibration curve is shown in Figure (15). The response is linear with hydrocarbon concentration, presented in units of ppmC, that is, the number of hydrogenated carbon atoms in parts per million.

Calibration of the Beckman Model 864 CO analyzer was accomplished using standard gases with 2530 ppm, 1550 ppm, 608 ppm, 305 ppm and 64 ppm CO in nitrogen. The calibration curve is shown in Figure (15).

The gases used for calibration of the Beckman Model 864 CO_2 analyzer contained 15.3%, 10.0%, 4.72% and 2.0% CO_2 in nitrogen. The analyzer calibration curve is slightly nonlinear as shown in Figure (15). The Beckman Model 951 NO/NO_x analyzer was calibrated using standards containing 411 ppm, 197 ppm, 91 ppm and 52 ppm NO_x in nitrogen.

The gas analysis instruments were calibrated once each week using the entire set of standard gases. Zero gas and span gas were passed through all instru-

ments immediately prior to each test and instrument output recorded on the same data roll which was used for the subsequent test run.

For the fuel distribution measurements, the following equation (in conformance with SAE ARP-1256) was used:

$$f/a = \frac{CO_2 + (CO + UHC) \times 10^{-4}}{208.1 - 2.04 \times 10^{-4} CO - 0.48 CO_2} \quad (1)$$

The measured volume fractions expressed as ppm of CO, hydrocarbons and NO_x are converted into emission indices (grams of component per kilograms of fuel) using the following expressions:

$$E_{CO} = \frac{CO\ (1 + f/a)}{1034\ f/a} \quad (2)$$

$$E_{HC} = \frac{HC\ (1 + f/a)}{2069\ f/a} \quad (3)$$

$$E_{NO_x} = \frac{NO_x\ (1 + f/a)}{630\ f/a} \quad (4)$$

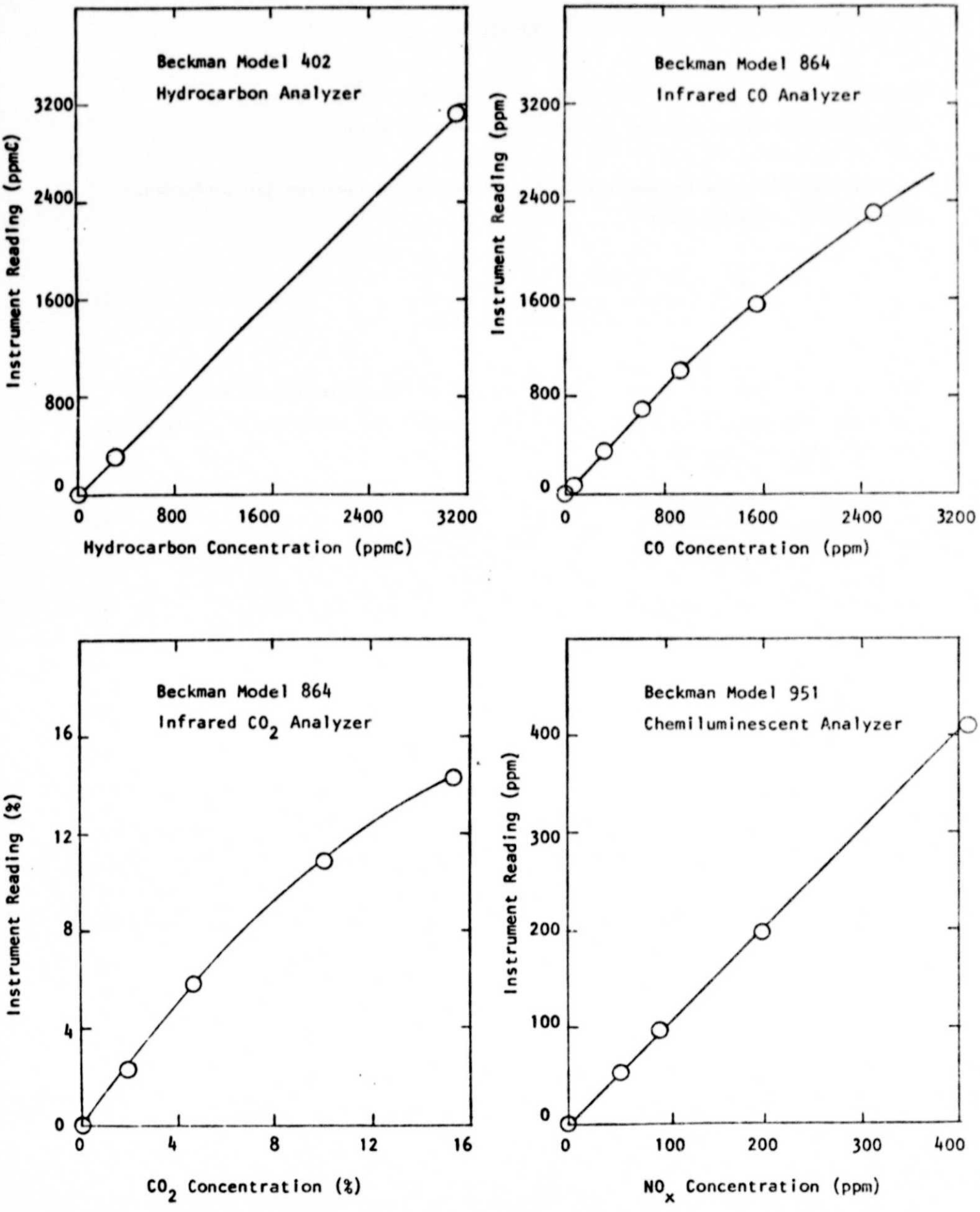

FIGURE 15. GAS ANALYSIS INSTRUMENT CALIBRATION CURVES

APPENDIX B

FUEL INJECTOR PRESSURE DROP CHARACTERISTICS

The variation of fuel injector pressure drop with fuel flow rate is plotted in Figure (16) for all operating conditions. Within the range covered by these tests, fuel flow rate varies as the square root of the fuel injector pressure drop. For a given pressure drop, the fuel flow rate is independent of the reference Mach number at all the three inlet temperatures.

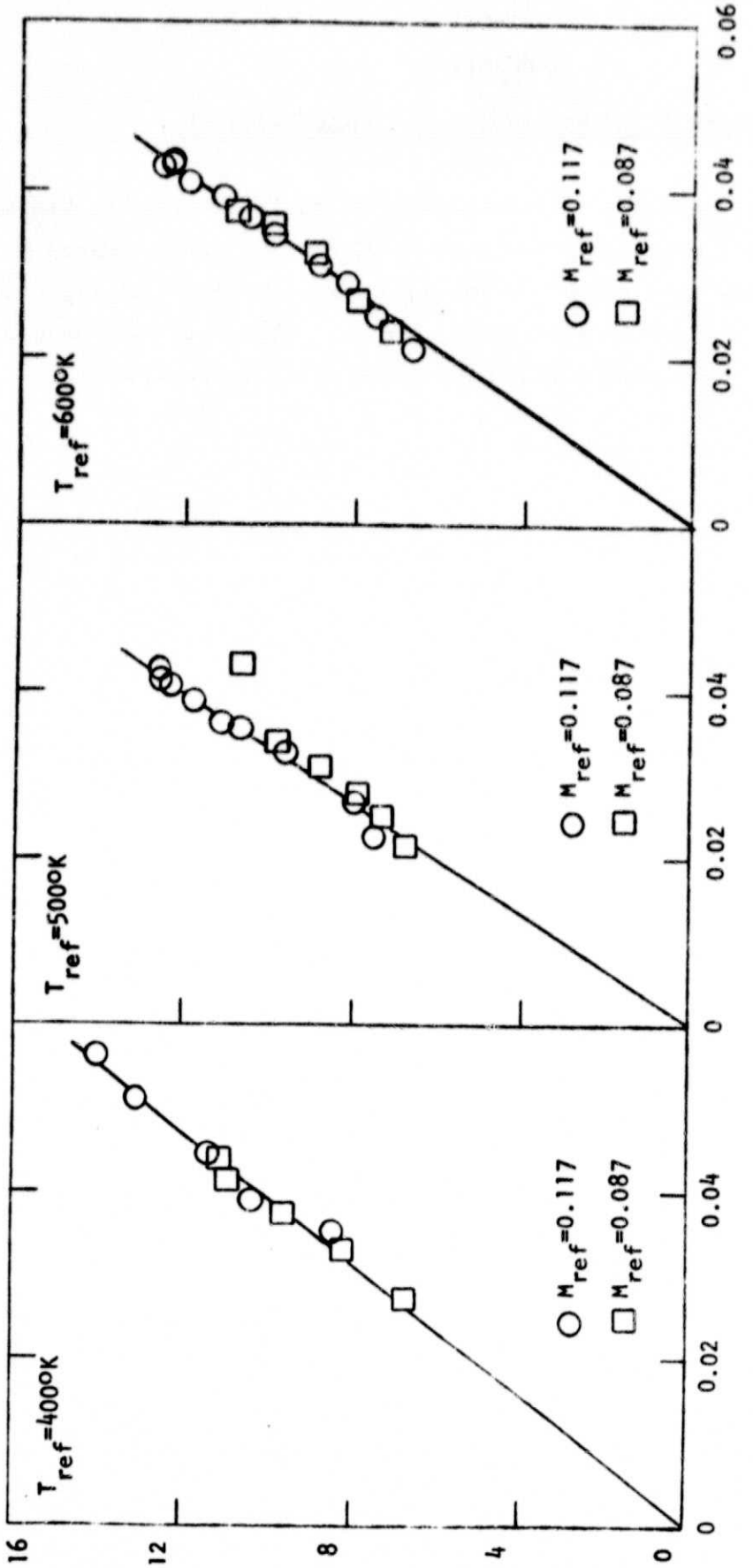

FIGURE 16. VARIATION OF FUEL INJECTOR PRESSURE DROP WITH FUEL FLOW RATE

REFERENCES

1. Westmoreland, J. S. and Godston, J., "VCE Testbed Program - Planning and Definition Study Final Report," NASA CR-135362, (1978).

2. Roffe, G., "Development of a Catalytic Combustor Fuel/Air Carburetion System," AFAPL-TR-77-19, Air Force Aero-Propulsion Laboratory, Air Force Systems Command, Wright Patterson Air Force Base, Ohio, (1977).

3. Chelko, L. J., "Penetration of Liquid Jets into a High-Velocity Airstream," NACA RM E50F21, (1950). (Also NACA Report 1300, 1957).

4. Roffe, G. and Venkataramani, K. S., "Emission Measurements for a Lean Prmixed Propane/Air System at Pressures to 30 Atmospheres," NASA CR-159421, June 1978.

TR 251

DATA SUMMARY

Emissions Data

T_{ref}	M_{ref}	ϕ (Metered)	CO_2 %	NO_x ppm	CO ppm	HC ppmC	E_{NO_x} g/kg-fuel	E_{HC} g/kg-fuel
600°K	0.087	0.859	6.93	50.80	>5000	2794	1.47	24.6
		0.820	6.50	44.26	>5000	5122	1.34	47.1
		0.742	7.17	53.82	>5000	6472	1.79	65.4
		0.605	8.65	95.56	>5000	2421	3.85	29.7
		0.527	9.33	111.90	>5000	2025	5.15	28.4
600°K	0.117	0.735	8.45	72.70	>5000	4330	2.43	44.1
		0.721	8.37	75.00	>5000	4727	2.56	49.1
		0.728	8.20	73.84	>5000	5051	2.49	51.9
		0.686	8.58	75.00	>5000	4005	2.68	43.6
		0.649	9.05	81.92	>5000	2526	3.09	29.03
		0.614	9.44	83.07	>5000	1804	3.30	21.8
		0.580	9.68	81.34	>5000	1443	3.42	18.5
		0.519	9.58	76.15	>5000	1137	3.56	16.2
		0.476	8.96	62.31	>5000	1137	3.17	17.6
		0.410	8.51	46.84	>5000	1642	2.76	29.4
		0.346	5.45	16.44	>5000	2291	1.14	48.4
500°K	0.087	0.885	7.45	41.53	>5000	468.0	1.17	4.00
		0.690	7.80	46.90	>5000	331.5	1.67	3.59
		0.644	8.20	51.33	>5000	253.5	1.95	2.93
		0.637	7.77	49.93	>5000	296.4	1.92	3.47
		0.573	8.30	50.63	>5000	187.2	2.15	2.42
		0.513	9.0	59.03	>5000	163.8	2.79	2.36
		0.435	8.48	56.00	>5000	163.8	3.11	2.77

DATA SUMMARY (Continued)

Emissions Data

T_{ref}	M_{ref}	ϕ (Metered)	CO_2 %	NO_x ppm	CO ppm	HC ppmC	E_{NO_x} g/kg-fuel	E_{HC} g/kg-fuel
500°K	0.117	0.637	8.03	41.78	>5000	1950	1.60	22.8
		0.653	7.84	42.92	>5000	2282	1.61	26.05
		0.627	7.84	42.92	>5000	2535	1.67	30.12
		0.595	7.74	42.92	>5000	2574	1.76	32.11
		0.558	7.74	44.52	>5000	2886	1.94	38.30
		0.537	7.88	45.66	>5000	2984	2.07	41.20
		0.502	8.10	43.15	>5000	2964	2.08	43.60
		0.412	6.35	22.83	>5000	2516	1.33	44.80
		0.412	6.17	19.46	>5000	2282	1.14	40.60
		0.344	4.92	13.35	>5000	1541	0.93	32.70
400°K	0.087	0.805	6.87	41.31	>5000	596.1	1.27	5.57
		0.758	7.26	41.77	>5000	12920	1.36	128.0
		0.685	6.51	30.99	>5000	8147	1.11	88.8
		0.603	6.41	28.00	>5000	8147	1.13	100.4
		0.496	6.73	27.31	>5000	4371	1.33	65.1
400°K	0.117	0.769	5.48	43.38	>5000	0	1.39	0
		0.700	5.20	43.61	>5000	0	1.53	0
		0.604	5.20	40.63	>5000	0	1.64	0
		0.529	5.74	32.59	>5000	0	1.50	0
		0.479	5.74	28.23	>5000	0	1.425	0

DATA SUMMARY

Emissions Data

T_{ref}	M_{ref}	Radial Distance cm	ϕ	CO_2 %	NO_x ppm	CO ppm	HC ppmC	E_{NO_x} g/kg-fuel	E_{HC} g/kg-fuel
				Cruise Condition					
604°K	0.087	-4.35	0.54	2.77	6.00	2260	195.0	0.26	2.60
		-2.9		3.10	8.19	1820	195.0	0.37	2.65
		-1.45		4.37	35.2	2400	585.1	1.57	7.97
		0		4.47	45.15	>5000	1127	2.11	16.1
		1.45		6.55	113.5	>5000	1019	5.07	13.9
		2.9		8.01	113.5	>5000	1019	5.07	13.9
		4.35		9.60	145.1	>5000	931.8	6.54	12.8
		-4.35	0.69	2.80	2.39	1610	550.5	0.095	6.61
		-2.9		3.05	8.95	950	293.6	0.320	3.15
		-1.45		4.55	25.29	>5000	550.5	0.90	5.95
		0		4.25	26.25	>5000	807.4	1.0	9.34
		1.45		5.0	48.67	>5000	715.7	1.88	8.43
		2.9		5.0	27.43	1215	1229	1.06	14.5
		4.35		9.20	53.21	>5000	807.4	2.08	9.64
		-4.35	0.76	3.20	9.19	1160	4294	0.30	42.22
		-2.9		3.28	12.05	1230	4844	0.39	47.6
		-1.45		4.60	21.00	>5000	4753	0.68	46.7
		0		3.60	16.7	>5000	4294	0.55	43.2
		1.45		4.20	32.21	>5000	3854	1.04	37.9
		2.9		6.12	7.76	>5000	4588	0.25	45.8
		4.35		9.10	78.15	>5000	3285	2.51	32.1
				Take-Off Condition					
430°K	0.117	-4.35	0.58	1.80	9.17	>5000	0	0.38	0
		-2.9		2.78	7.91	>5000	0	0.33	0
		-1.45		4.58	14.67	>5000	0	0.61	0
		0		2.9	30.11	>5000	0	1.26	0
		1.45		4.7	29.72	>5000	0	1.24	0
		2.9		5.22	34.35	>5000	0	1.44	0
		4.35		9.55	60.6	>5000	0	2.53	0
		-4.35	0.63	2.05	11.19	>5000	64.32	0.42	0.74
		-2.9		3.08	8.97	>5000	221.9	0.35	2.62

DATA SUMMARY (Continued)

Emissions Data

T_{ref}	M_{ref}	Radial Distance cm	ϕ	CO_2 %	NO_x ppm	CO ppm	HC ppmC	E_{NO_x} g/kg-fuel	E_{HC} g/kg-fuel
				Take-Off Condition (Continued)					
430°K	0.117	-1.45	0.63	4.88	12.55	>5000	302.3	0.49	3.57
		0		2.18	38.6	>5000	43.42	1.51	0.52
		1.45		4.05	35.51	>5000	257.3	1.39	3.06
		2.9		3.78	47.48	>5000	225.1	1.86	2.68
		4.35		8.28	84.92	>5000	884.4	3.29	10.44
		-4.35	0.70	1.62	16.6	>5000	1415	0.58	14.99
		-2.9		3.34	12.16	>5000	1544	0.43	16.52
		-1.45		4.28	11.58	>5000	1624	0.41	17.38
		0		1.52	60.22	>5000	434.2	2.12	4.65
		1.45		3.30	51.72	>5000	627.1	1.82	6.71
		2.9		2.55	78.74	>5000	530.6	2.77	5.68
		4.35		6.15	103.4	>5000	1399	3.56	14.7